Reinforcing mechanism of Geosynthetics on bearing capacity problems – model tests and numerical simulations

Mécanismes de renforcement de la capacité portante par géosynthétiques – essais sur modèles réduits et modélisations numériques

T. Nakai, H. M. Shahin, A. Watanabe and S. Yonaha
Nagoya Institute of Technology, Nagoya, Japan

ABSTRACT

In this paper, bearing capacity problem of reinforced-soil ground is investigated and the reinforcing mechanism is clarified through two-dimensional laboratory model tests and the corresponding numerical analyses. The numerical analyses are carried out using elastoplastic subloading t_{ij} model. Changing the installation depth, length and skin friction of the reinforcements several tests are carried out. It is revealed that the effectiveness of reinforcement, bearing capacity of reinforced ground, mainly depends on the position of reinforcement and its skin friction. There is almost no extra reinforcement effect is seen when it is placed deeper than a certain depth. The results obtained from the numerical analyses show very good agreement with the results of the model tests.

RÉSUMÉ

Dans cet article, la portance des sols renforcés est étudiée et le mécanisme de renforcement est mis en évidence par des essais de laboratoire sur modèle réduit et les analyses numériques correspondantes. Les modélisations numériques ont été réalisées à l'aide d'un modèle élasto-plastique tij à sous chargement. Plusieurs tests ont été réalisés en faisant varier la profondeur de mise en place des renforcements, leur longueur ainsi que leur frottement de surface. Lorsqu'il est mis en œuvre au-delà d'une certaine profondeur, le renforcement n'apporte pas d'effet particulier. Les résultats obtenus à partir des modélisations numériques ont montré une très bonne adéquation avec les résultats expérimentaux.

Keywords : Geosynthetics, soil-reinforcement, bearing capacity, finite element analysis

1 INTRODUCTION

To reduce ground deformation and earth pressure of the ground and to increase bearing capacity, reinforced earth method is adopted using Geosynthetics such as Geogrid and Geotextile. However, till now the reinforcement mechanism for establishing a rational design method of reinforced-soil ground is not fully understand. In this paper, bearing capacity problem of reinforced-soil ground is investigated and the reinforcing mechanism is clarified through two-dimensional laboratory model tests and the corresponding numerical analyses. In the model tests, mass of aluminum rods is used as ground which shows almost the same mechanical characteristics of sandy soil, and tracing paper having almost no bending stiffness is used as reinforcement material. The numerical analyses are carried out using elastoplastic subloading t_{ij} model (Nakai & Hinokio, 2004). The model can consider influence of intermediate principal stress on the deformation and strength of soils, dependence of the direction of plastic flow on the stress paths, influence of density and/or confining pressure on the deformation and strength of soils.

2 LAYOUT OF MODEL TESTS AND NUMERICAL ANALYSES

Figure 1 shows a schematic diagram of 2D model test apparatus. In the model tests, mass of aluminum rods, having diameters of 1.6 and 3.0mm and mixed in a ratio of 3:2 in weight, is used as ground which shows almost the same mechanical characteristics of sandy soil. The unit weight of the aluminum rod mass is 20.4kN/m^3, and the length is 5.0cm. Vertical load is applied at the center of a flat foundation (width of B=12cm) using a motor. A slider which permits the movement of the loading rod in the horizontal direction and a load cell for measuring the magnitude of load are set in the loading system.

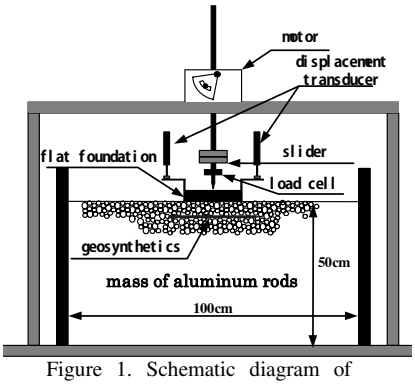

Figure 1. Schematic diagram of Apparatus

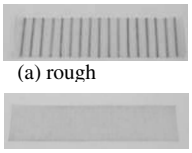
(a) rough

(b) smooth

Figure 2. Types of reinforcements

Vertical displacement and rotation of the foundation are measured with setting two displacement transducers at the two ends of the foundation. Tracing paper having almost no bending stiffness is used as reinforcement material, which is set underneath the foundation changing the installation depths (D). Four sets of reinforcement lengths L=36cm (L/B=3), L=24cm (L/B=2), L=12cm (L/B=1) and L=6cm (L/B=0.5) are considered. As shown in Fig.2, two kinds of frictional conditions of geosynthetics are employed – the first type where aluminum rods having diameter of 1.6mm are glued at both sides of the tracing paper to simulate rough condition (frictional angle between the ground and the reinforcement $\delta=20^0$), and the second type where the smooth behavior of reinforcement is considered without gluing aluminum rods on the tracing paper (frictional angle between the ground and the reinforcement $\delta=8^0$). Changing the installation depth (D), the length (L) and the skin friction (δ) of the reinforcements 13 tests patterns are considered (Table 1). Taking photographs of the model ground with a digital camera the deformation of the ground is captured.

Proceedings of the 17th International Conference on Soil Mechanics and Geotechnical Engineering
M. Hamza et al. (Eds.)

doi:10.3233/978-1-60750-031-5-917

Table 1. Test patterns

δ	L/B		D/B			
No reinforcement						
Rough reinforcement δ=20^0	1/2		1/4			
	1		1/4			
	2	0	1/8	1/4	1/2	1
	3		1/4			
Smooth reinforcement δ=8^0	2		1/8	1/4	1/2	1

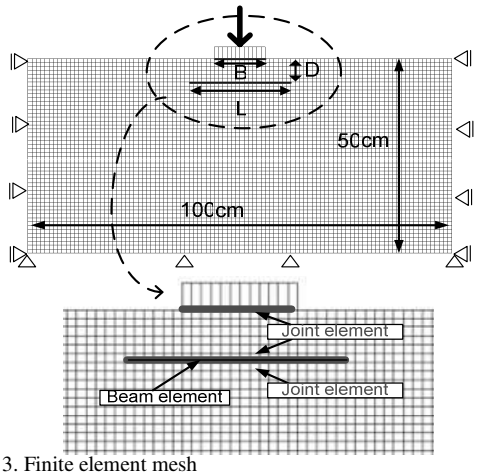

Figure 3. Finite element mesh

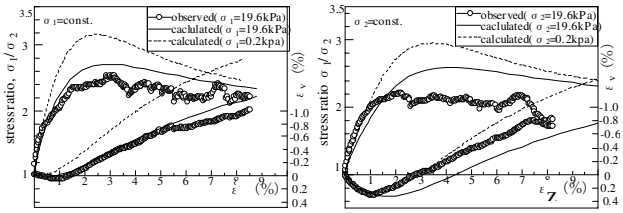

Figure 4. Stress-strain-dilatancy relation of aluminum rods mass

Table 2. Parameters of soil materials

Parameters	Value
λ	0.0080
κ	0.0040
N (e_{NC} *at p=98kPa & q=0kPa*)	0.30
$R_{CS}=(\sigma_1/\sigma_3)_{CS(comp.)}$	1.80
β	1.20
ν_e	0.20
a	1300

Figure 3 represents the mesh used in the numerical analyses. The finite element analyses are carried out with FEMtij-2D considering plane strain drained condition for the same scale of the model tests using elastoplastic subloading t_{ij} model (Nakai & Hinokio, 2004). Isoparametric 4-noded elements are used for soil elements, and elastic beam elements are used to simulate reinforcements. The frictional behavior between the reinforcement and soil, and the foundation and soil, is modeled employing elastoplastic joint element (Nakai, 1985). Model parameters for the aluminum rod mass are shown in Table 2. The parameters are fundamentally the same as those of the Cam clay model except the parameter *a,* which is responsible for the influence of density and confining pressure. The parameter β represents the shape of yield surface. The parameters can easily be obtained from traditional laboratory tests. Figure 4 shows the results of the biaxial tests for the mass of aluminum rods used in the model tests. From the stress-strain behavior of the element tests simulated with subloading t_{ij} model, it is noticed that this model can express the dependency of stiffness, strength and dilatancy on the density as well as on the confining pressure.

Figure 5 shows the computed results of elastoplastic joint element (Nakai, 1985). It is found in the figure that almost no slippage (w_s) is observed at the interface till the ratio of shear to normal stresses (P_s/P_n) reaches the value which is equal to tanδ. After P_s/P_n becomes tanδ, slippage occurs maintaining P_s/P_n is equal to tanδ. Therefore, the interface model can describe the mechanical behavior of interface boundary. The frictional angles between the reinforcement and soil, and foundation and soil which are obtained in experiments are used in the numerical analyses. Table 3 represents the parameters of reinforcements.

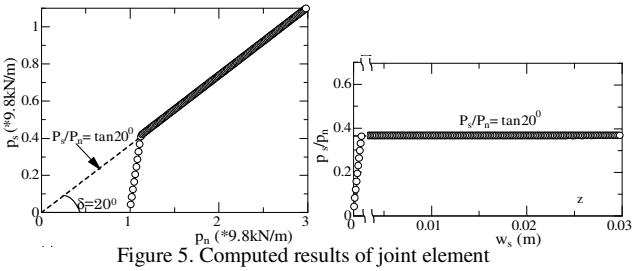

Figure 5. Computed results of joint element

Table 3. Parameters of reinforcement

beam element(/cm)	
EI	1.34×10^{-7}N·m^2
EA	1.31×10^{3}N

3 RESULTS AND DISCUSSIONS

3.1 *Influence of installation depth of reinforcement*

Figure 6 shows the observed and computed bearing capacity for different installation depths where the reinforcement length is 24cm. The vertical axes represent vertical load q_v which is divided by $\gamma B/2$, while abscissas show normalized vertical displacement which is normalized by the width of the foundation (B). The figures also show the results of no reinforcement. The influence of reinforcement can not be expected when the installation depth is deeper than a certain depth (D/B is greater than 1/2). In addition, when the reinforcement is placed on the ground surface just below the foundation, there is almost no effect of the reinforcements except the friction coefficient of the foundation. The numerical analyses capture well the influence of the installation depth in the same way as the model tests.

Figure 7 represents the distributions of bending moment and axial force of reinforcements. It is seen that the bending moment is almost zero in all cases as expected, however, either a big range of larger axial force is distributed in the central part of the reinforcement or the value of axial force in the central part of the

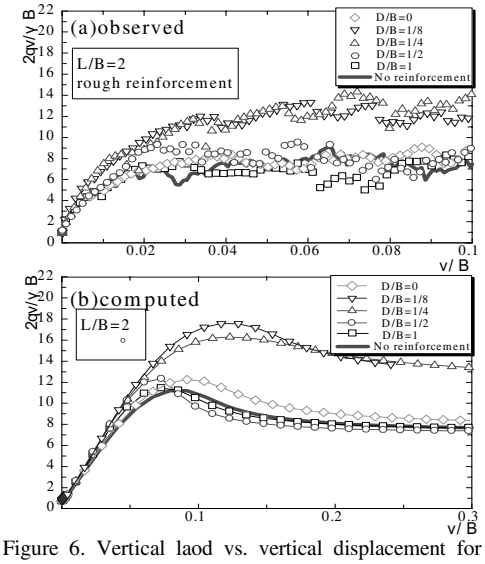

Figure 6. Vertical laod vs. vertical displacement for different installation depths of reinforcement

reinforcement becomes remarkably high where the effect of reinforcement exists (D/B=1/8, 1/4). Figure 8 shows observed and computed shear strain distributions of the ground while the load approaches to peak strength (for the model test it is at v/B=0.04, while it is at v/B=0.1 for the analysis). The distribution of shear strain of the model tests are obtained from the simulation of Particle Image Velocimetry (PIV) technique taking two photographs before and after loading. The top most figure represents the results of the ground without reinforcement. It is seen that where the effect of reinforcement is the most (D/B=1/8), a zone of large shear strain spreads vertically below the foundation compare to no reinforcement. For D/B=1/2 and 1, where there is almost no effect of reinforcement, the zone of large shear strain does not spread vertically below the foundation. Especially, for D/B=1.0 the distribution of shear strain is almost the same as the case of no reinforcement, in this case reinforcement does not take part in ground improvement. The computed results describe well the differences of the shear strain distribution as observed in the model tests.

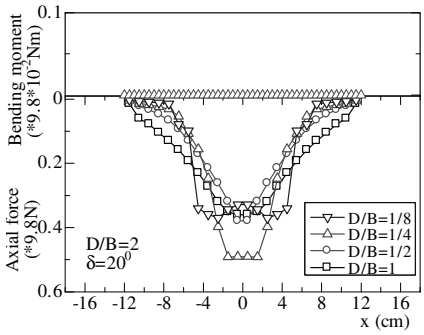

Figure 7. Computed bending moment and axial force for different installation depths of reinforcement

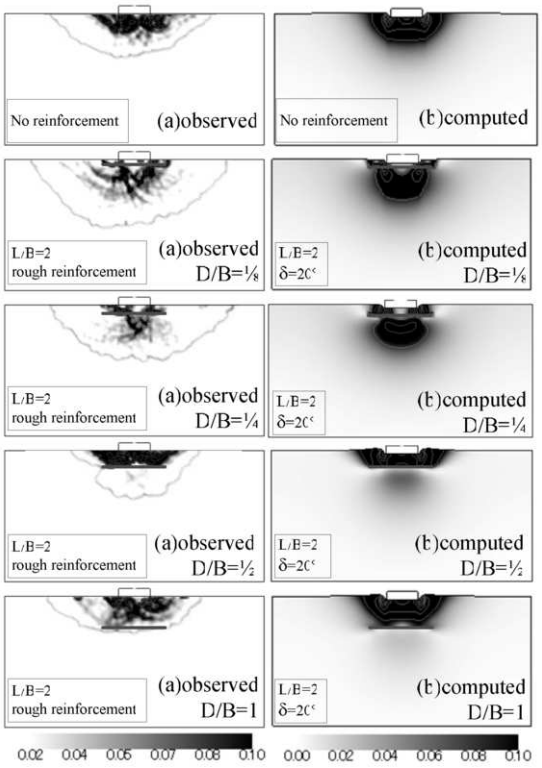

Figure 8. Shear strain distribution for different installation depths of reinforcement

3.2 *Influence of reinforcement length*

The influence of reinforcement is investigated for several reinforcement lengths keeping a constant installation depth (D/B=1/4). The similar graphs that are illustrated in the previous section for different installation depths will be shown in this section. Figure 9 shows the relationships of load-displacement for different reinforcement lengths. It is observed that even for L=6cm (L/B=1/2) there are some effects of reinforcing on the bearing capacity of the ground, however, almost no differences of reinforcement effects on bearing capacity are observed for L/B greater than 1.0. The numerical analyses perfectly capture the results of the model tests.

Figure 10 represents distributions of bending moment and axial force of reinforcements. Almost the same distribution of axial force is seen for L/B greater than 1.0, which describes the mechanism of reinforcement mentioned above. Figure 11

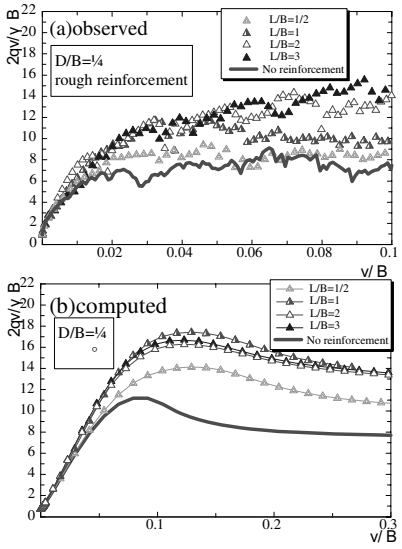

Figure 9. Vertical laod vs. vertical displacement for different the distributions of shear strain of the ground similar to Fig.8. (see Fig.8, for the results of no reinforcement and L/B=2.0). lengths of reinforcement

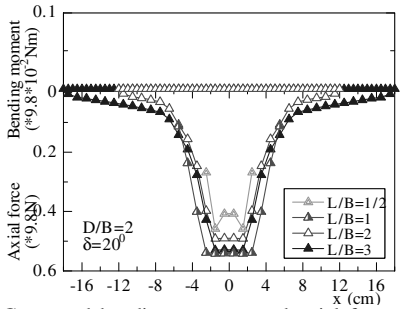

Figure 10. Computed bending moment and axial force for different lengths of reinforcement

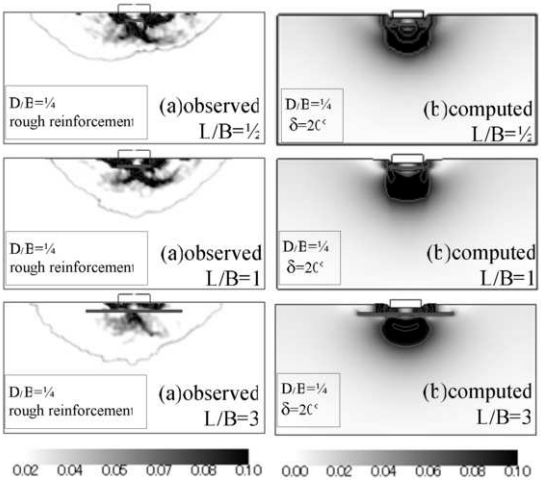

Figure11. Shear strain distribution for different lengths of reinforcement

With the increase of reinforcement effect a zone of large shear strain spreads vertically below the foundation. The same effect of reinforcement can be expected when L/B is greater than 1.0.

3.3 *Influence of friction angle of reinforcement*

In the two previous sections the friction angle (δ) was 20^0. In this section, the effects of friction angle will be discussed for the same condition illustrated in section 3(a) (L=24cm) except using different friction angle ($\delta=8^0$). Here, the surface of reinforcement (tracing paper) is smooth, i.e., there is no aluminum rods glued on the tracing paper. The relationships of load-displacement is shown in Fig.12. Figure 13 illustrates the distribution of bending moment and axial force. Figure 14 represents the distributions of shear strain of the ground (see Fig.8, for the results of no reinforcement). Comparing Figs.6 and 12, it is revealed that in the smaller friction angle the reinforcement effect decreases even for the same stiffness of the reinforcement. From Fig.12, it is seen that if the reinforcement is installed at an appropriate depth (for instance D/B=1/8) the bearing capacity of the ground increases even for the smooth surface of reinforcement. A reverse effect can also be seen (for example D/B=1/2) depending on the installation depth in the case of smaller friction angle. Almost no reinforcing effect is observed in D/B=1 for both types of friction angles. The numerical analyses grasp well the phenomenon of reinforcing effect for different friction angles.

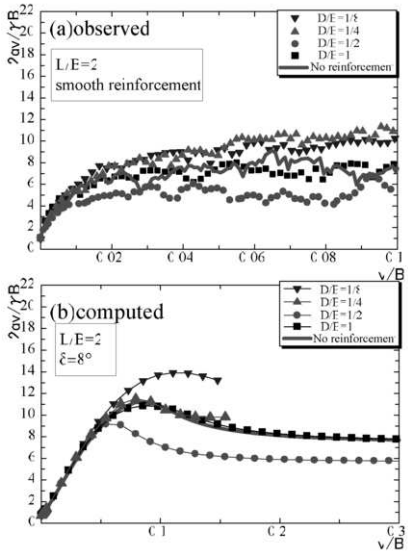

Figure 12. Vertical laod vs. vertical displacement: smooth reinforcement

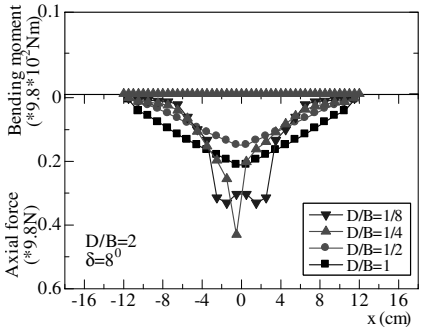

Figure 13. Computed bending moment and axial force: smooth reinforcementt

From Fig.13 it is found that the axial force for D/B=1/2 is smaller than that for D/B=1, therefore a negative effect of reinforcement for D/B=1/2 can be speculated. From Figs.7, 10 and 13, it is observed that though the axial force is smaller at the edges, it increases at the central part of the reinforcement for the cases where reinforcing effect exists. Shear strain develops to a wider and deeper region even for the smooth reinforcement in D/B=1/8 where reinforcing effect exists (Fig.14). On the other hand, for the smooth reinforcement in D/B=1/2, where negative reinforcing effect exists, the region of larger shear strain is shallower than that for no reinforcement. This is because, slippage occurs on the top surface of the reinforcement before developing a zone of shear strain vertically below the foundation. Hence, larger shear strain concentrates near the ground surface. The numerical analyses can produce well the mechanism of shear strain distribution of the model tests.

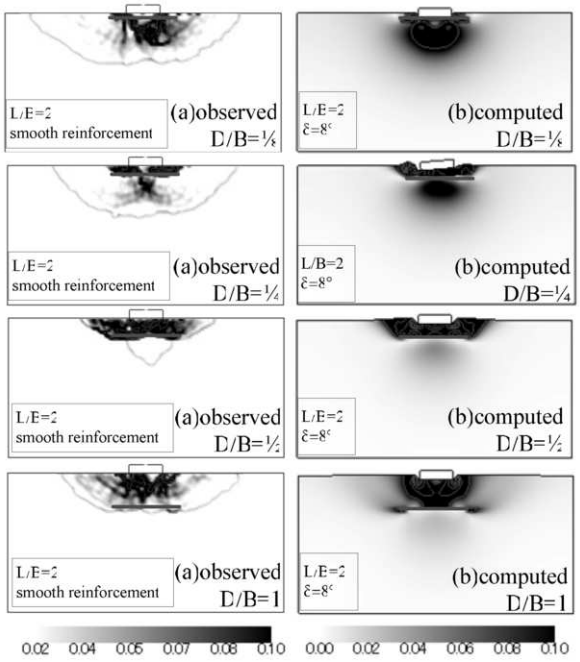

Figure 14. Shear strain distribution: smooth reinforcement

4 CONCLUSIONS

The bearing capacity of soil-reinforcement using Geosynthetics has been investigated with laboratory model tests and the corresponding numerical analyses. It is revealed that the effectiveness of reinforcement mainly depends on the position of reinforcement and its skin friction. Almost no extra reinforcement effect is seen when it is placed deeper than a certain depth (D/B=1/2). Even a moderate effect of reinforcement is obtained for the reinforcement having smaller skin friction except for D/B=1/2 where a negative reinforcing effect is observed. Reinforcement length grater than the width of the foundation is preferable. A wider and deeper region of shear strain is confirmed during the effect of reinforcement. At that time, the maximum tensile force is developed at the central part of the reinforcement. The results obtained from the numerical analyses show very good agreement with the results of the model tests in all patterns, such as in different length of reinforcements, installation depth and skin friction of reinforcements. It can be concluded that if the mechanical properties of ground material, reinforcing material and skin friction of reinforcement are appropriately considered, and the soil-reinforcement is treated as an interaction problem of the soil and structure (soil and reinforcement), it is possible to explain the reinforcement mechanism properly with such model tests and numerical simulations.

REFERENCES

Nakai, T. 1985. Finite element computations for active and passive earth pressure problems of retaining wall. *Soils and Foundations*, 25(3), 98-112.

Nakai, T. and Hinokio, M. 2004. A simple elastoplastic model for normally and over consolidated soils with unified material parameters. *Soils and Foundations*. 44(2), 53-70.